Rheology : the Crystals Behind the Flow

Patrick Cordier
University of Lille, Villeneuve d'Ascq France

Mantle convection is special (compared to other dynamical processes which take place in the outer core or in the atmosphere) in that it is taking place in a solid medium. Mineral Physics studies conducted in the past years have yielded a mineralogical model of the Earth's mantle which satisfies the seismological constraints. The need for a rheological model of the mantle based on this mineralogy has appeared very early. However, this approach has faced very severe limitations. Indeed, the rheology of solids is much more complicated than with liquids (it is often strongly non-linear, and can involve a vast range of micrsocopic mechanisms). Important issues such as the influence of pressure or low strain-rates on the deformation mechanism of solids are still poorly understood. Moreover, the extreme P, T conditions prevailing in the mantle have been an obstacle to experimental investigations for a long time.

This situation has evolved significantly in the past few years. Outstanding breakthroughs have been achieved in the field of experimental deformation at high pressure. Well controlled deformation experiments can be conducted at conditions approaching those of the transition zone using the newly developed Deformation DIA and Rotational Drickamer Apparatus whereas higher pressures are accessible with the Kawai multianvil presses and the Diamond Anvil Cells. The development of in-situ stress and strain measurements using synchrotron sources have given to these experiments their complete dimension. Alternatively, it is now possible to address the issue of rheology from the numerical point of view. The difficulty here is that this property is intrinsically multiscale. Several approaches must be combined to take into account the physics involved at the atomic scale (quantum mechanics), at the mesoscopic scale (collective behaviour of defects), at the scale of the aggregate (continuum mechanics) and to make the link with mantle properties. These approaches will be briefly described.

Finally, these recent progresses will be illustrated by some ongoing research dealing with:

- Olivine (influence of pressure on plastic anisotropy, dislocation dynamics, texture formation)
- $MgSiO_3$ perovskite (slip systems, influence of orthorhombic distortions, behaviour within a polycrystalline aggregate with MgO)
- Post-perovskite (plastic shear anisotropy)

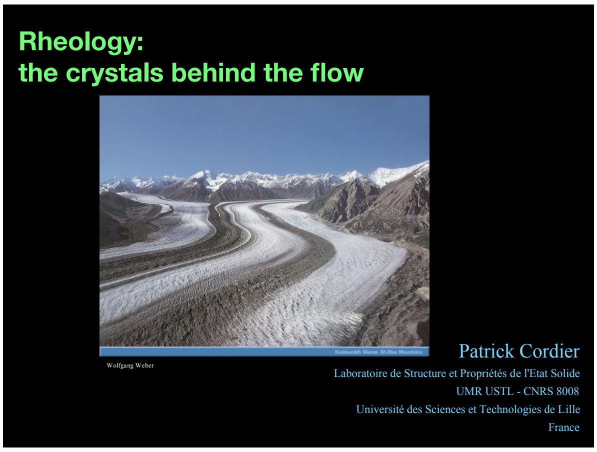
Rheology:
the crystals behind the flow
Wolfgang Weber
Patrick Cordier
Laboratoire de Structure et Propriétés de l'Etat Solide
UMR USTL - CNRS 8008
Université des Sciences et Technologies de Lille
France

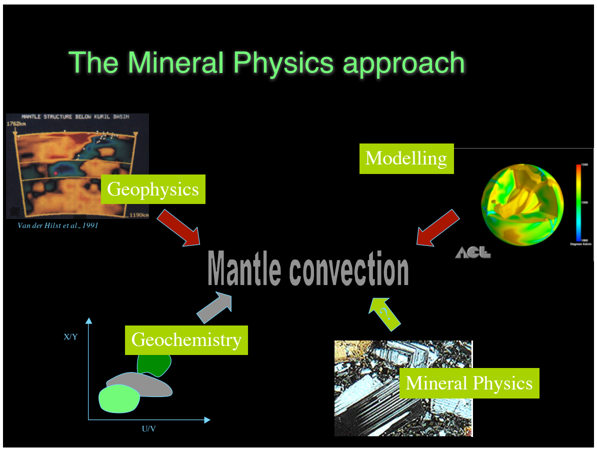
The Mineral Physics approach
Geophysics
Van der Hilst et al., 1991
Modelling
Mantle convection
Geochemistry
X/Y
U/V
Mineral Physics

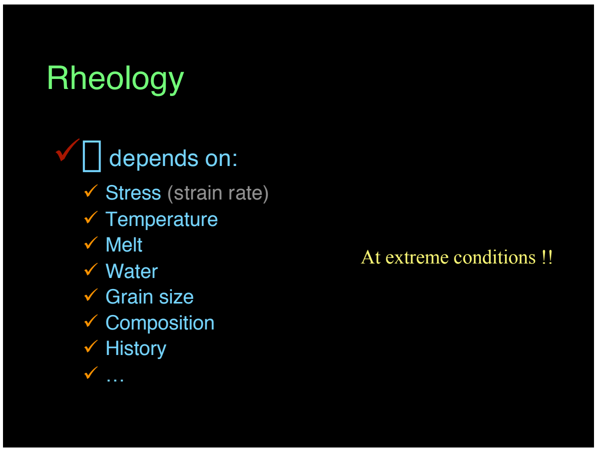
Rheology
depends on:
Stress (strain rate)
Temperature
Melt
Water
Grain size
Composition
History
…
At extreme conditions !!

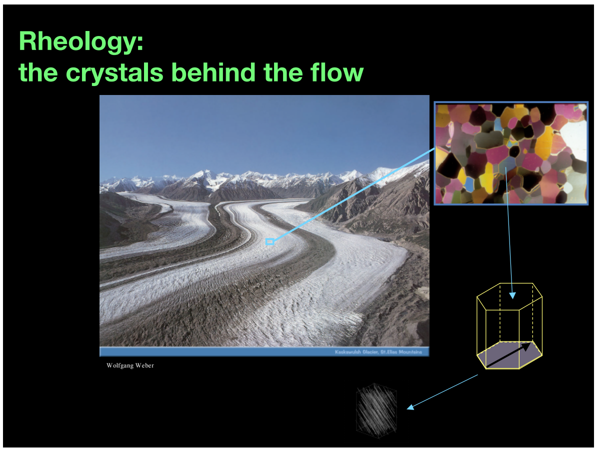
Rheology:
the crystals behind the flow
Wolfgang Weber

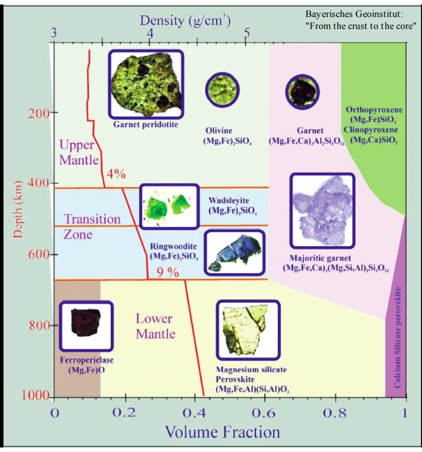

The experimental approach

Mechanical test

Galilée (Leyden 1638)

Constitutive equation:

$$\dot{\varepsilon} = A\sigma^n f_{O_2}^m a_{opx}^q \exp(-\Delta H / RT)$$

The usual tools of rock mechanics

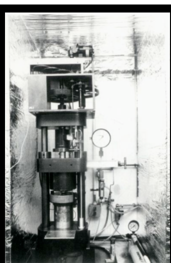

Griggs rig
P < 4 GPa

Paterson rig
P < 0.5 GPa

Rotational Drickamer Apparatus

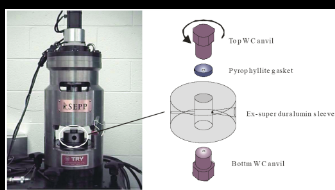

- P_{max} = 15 GPa
- T_{max} = 1800 K
- Thin disc (0.8 x 4 mm)
- Strain rate > 10^{-6} s^{-1}

Yamasaki & Karato (2001)

See poster P2

Deformation - DIA

- P_{max} = 15 GPa
- T_{max} = 2000 K
- Strain rate > 10^{-6} s^{-1}

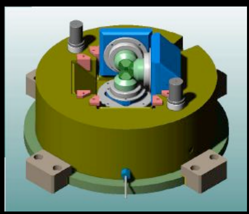

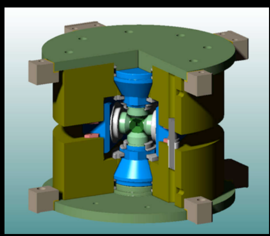

Y. Wang, W. Durham, Y. Getting
and D. Weidner (2003)

In situ measurements of strain and stress

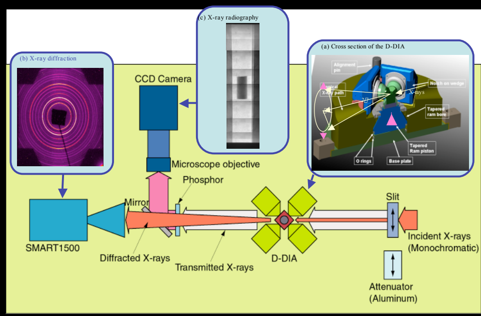

GSECARS/ University of Chicago

Multianvil experiments

- "Large" volumes: 1-12 mm^3
- P up to 26 GPa
- T up to 2500K

Bayerisches Geoinstitut

Olivine 11 GPa (H. Couvy)

Ringwoodite 22 GPa

Diamond anvil cell

- Small samples
- Heating

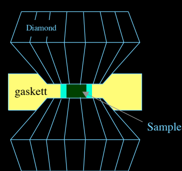

Perovskite $MgSiO_3$
30 GPa - RT
(coll. A. Dewaele)

An alternative: multiscale modelling

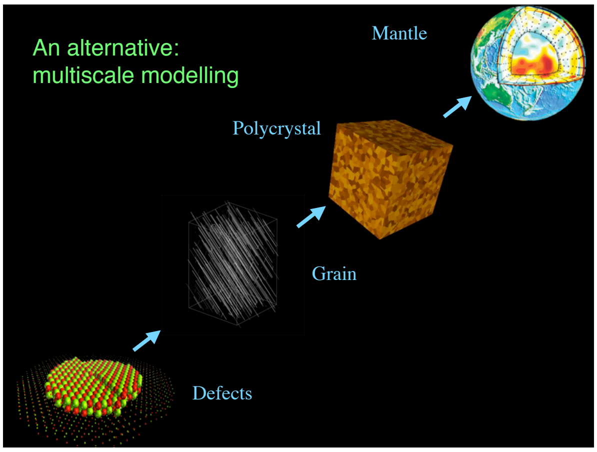

Plastic deformation

- ✓ produced by slip over crystallographic planes

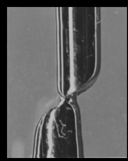

(Kubin, 1971)

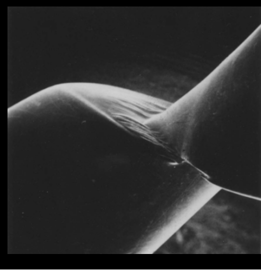

Plastic deformation

- ✓ produced by slip over crystallographic planes

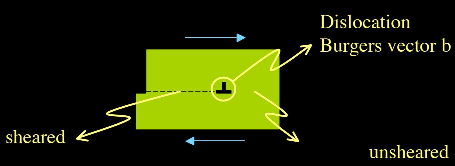

Multiscale modelling of plasticity

Crédit: A. Walker

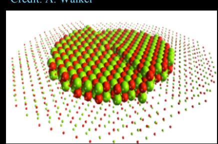

Atomic scale

- ✓ Quantum mechanics
- ✓ Dislocation core - bonding
- ✓ Plastic shear anisotropy

Multiscale modelling of plasticity

- Solid state physics
- Crystal defects (dislocations)

$\square = \square bv$

Scale: single crystal

3D dislocation dynamics - L. Kubin (ONERA)

Multiscale modelling of plasticity

- Solid state physics
- Crystal defects (dislocations)

$\square = \square bv$

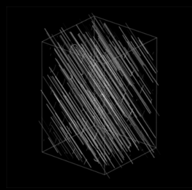

Scale: single crystal

3D dislocation dynamics - L. Kubin (ONERA)

Multiscale modelling of plasticity

Scale: polycrystal

- Continuum mechanics
- Complex strain and stress partitionning
- Self-consistent methods
  Finite elements
- Taking physics into account

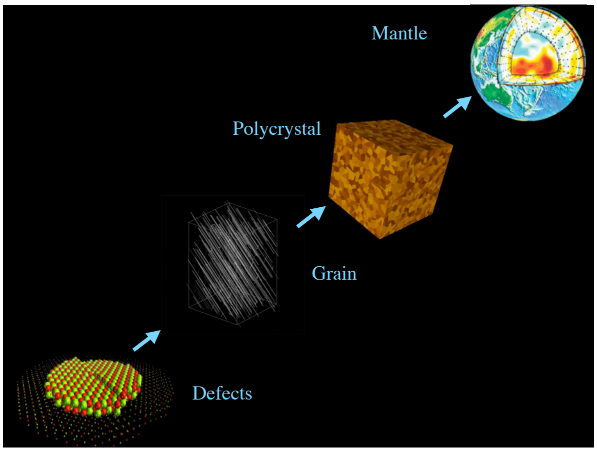

Anisotropy,… and anisotropy

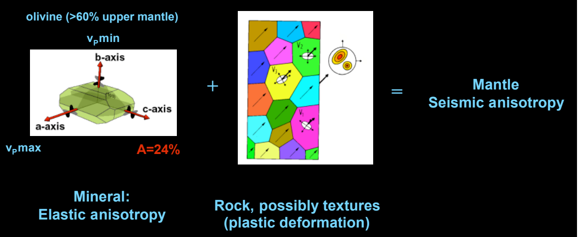

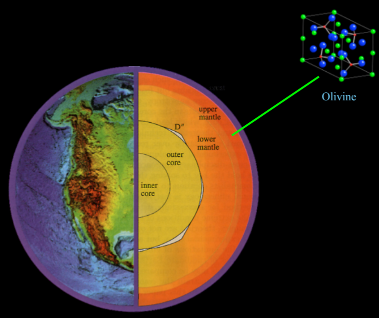

Olivine

✓ Slip systems

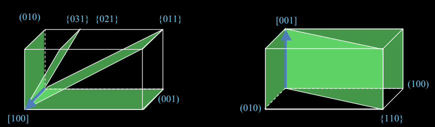

Deformation of forsterite at high-pressure

Shear deformation assembly
Karato & Rubie (1997)

Kawai Multianvil apparatus - Bayreuth

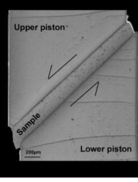

11 GPa - 1400°C

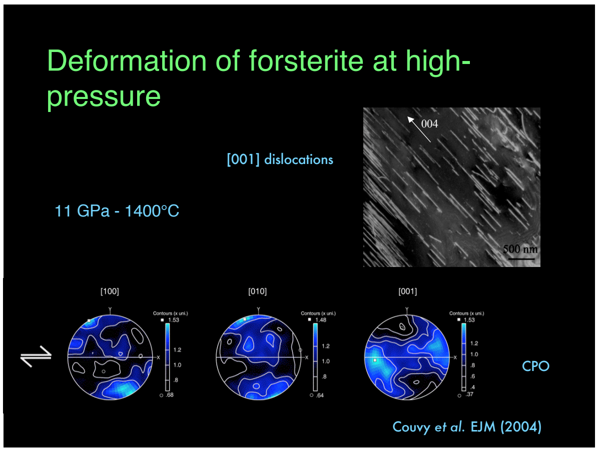

Deformation of forsterite at high-pressure
[001] dislocations
004
500 nm
11 GPa - 1400°C
[100]
[010]
[001]
CPO
Couvy et al. EJM (2004)

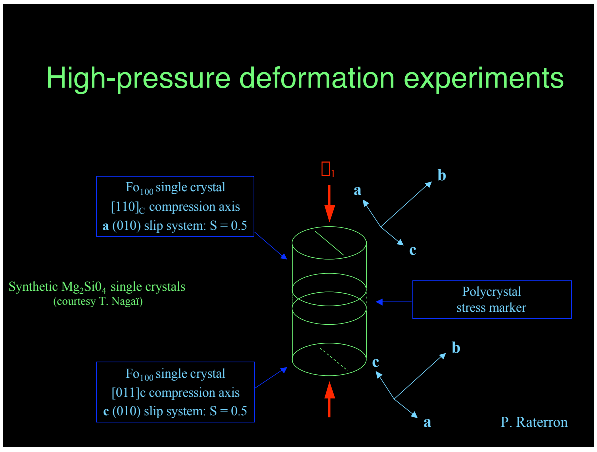

High-pressure deformation experiments
Fo100 single crystal
[110]C compression axis
a (010) slip system: S = 0.5
Synthetic Mg2Si04 single crystals
(courtesy T. Nagaï)
Polycrystal
stress marker
Fo100 single crystal
[011]c compression axis
c (010) slip system: S = 0.5
a
b
c
P. Raterron

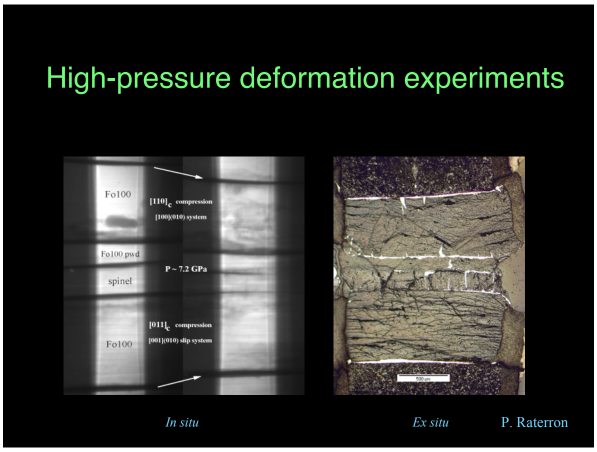

High-pressure deformation experiments
Fo100
[110]c compression
[100](010) system
Fo100 pwd
P ~ 7.2 GPa
spinel
[011]c compression
[001](010) slip system
Fo100
In situ
Ex situ
P. Raterron

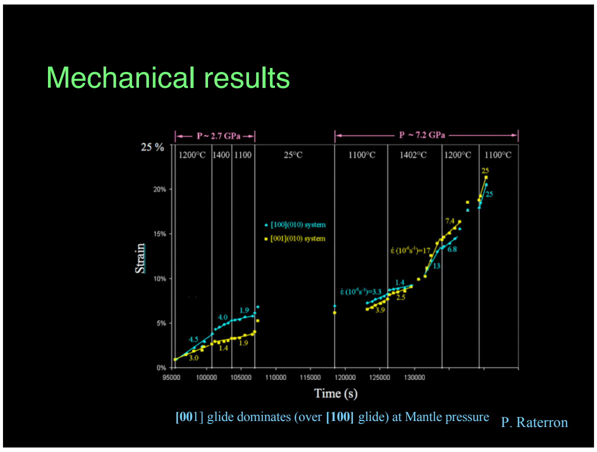

Mechanical results
P ~ 2.7 GPa
P ~ 7.2 GPa
1200°C
1400
1100
25°C
1100°C
1402°C
1200°C
1100°C
[100](010) system
[001](010) system
Strain
Time (s)
[001] glide dominates (over [100] glide) at Mantle pressure
P. Raterron

Mechanical results

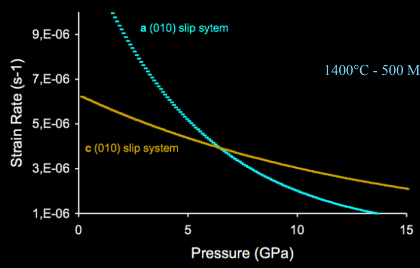

1400°C - 500 MPa

P. Raterron

Mechanical results

- ✓ Pressure has an influence on plastic deformation mechanisms

(Yannick, add this one to your list !)

- ✓ Why ?

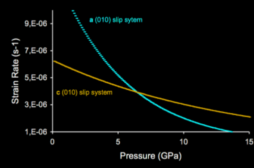

Modelling Plastic anisotropy

- ✓ Using Generalised Stacking Faults (GSF)

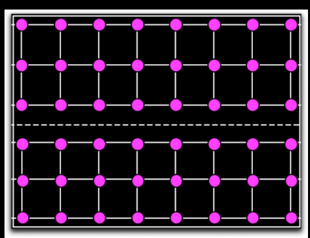

Dislocations and GSF’s

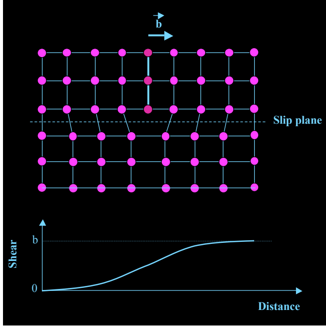

Edge dislocation

Distribution of shear in the vicinity of the dislocation core

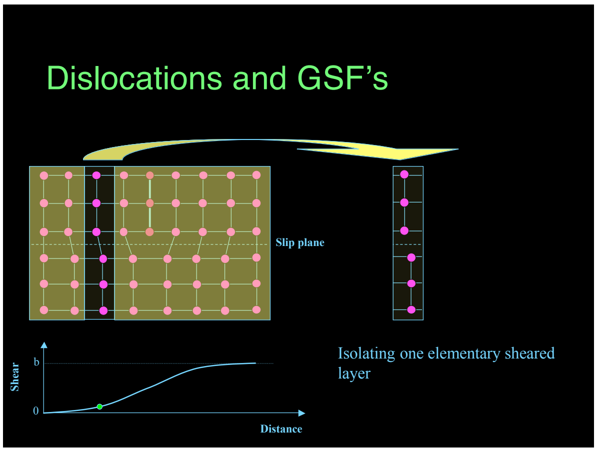
Dislocations and GSF's
Slip plane
Isolating one elementary sheared layer
Shear
b
0
Distance

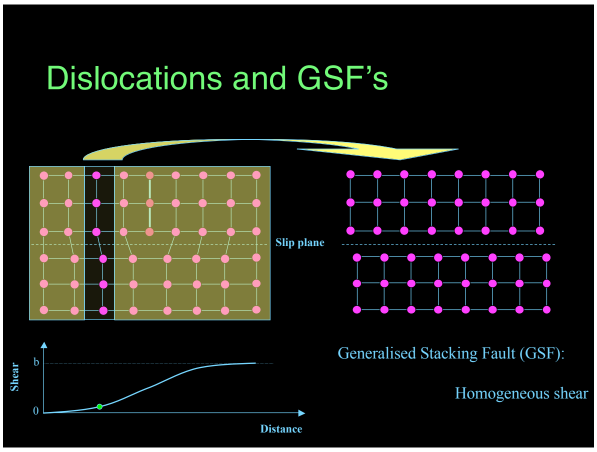
Dislocations and GSF's
Slip plane
Generalised Stacking Fault (GSF):
Homogeneous shear
Shear
b
0
Distance

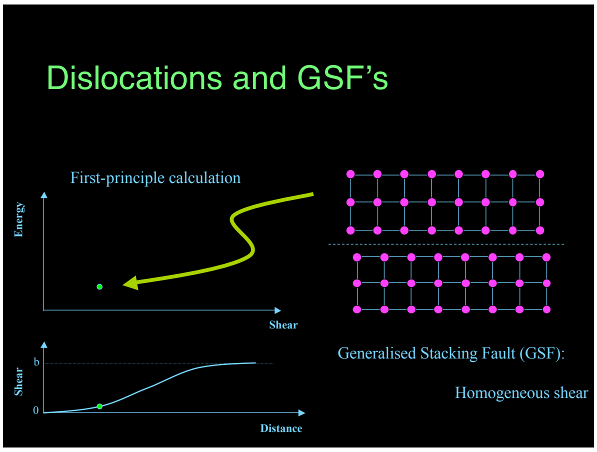
Dislocations and GSF's
First-principle calculation
Energy
Shear
Generalised Stacking Fault (GSF):
Homogeneous shear
Shear
b
0
Distance

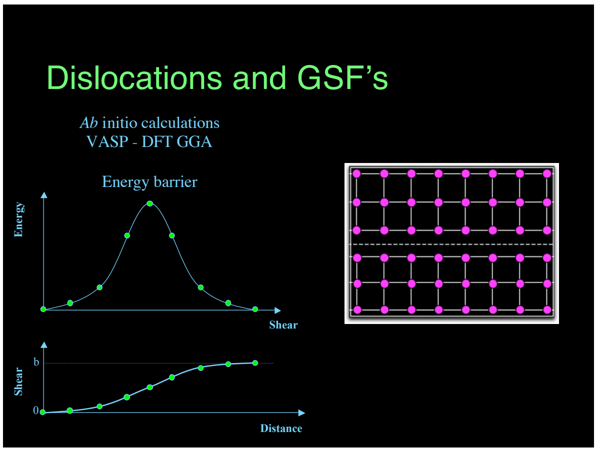
Dislocations and GSF's
Ab initio calculations
VASP - DFT GGA
Energy barrier
Energy
Shear
Shear
b
0
Distance

Dislocations and GSF's

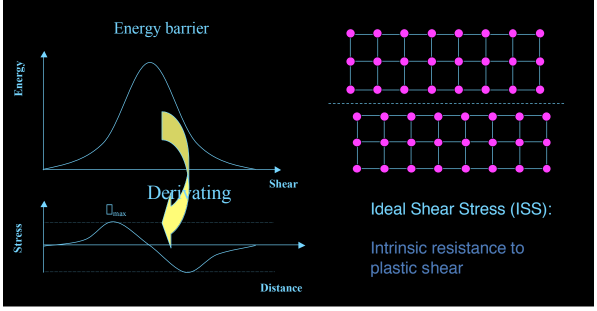

Ab initio calculations

V.A.S.P. (Vienna *Ab-initio* Simulation Program)

- DFT - GGA
- Ultrasoft pseudopotentials
  - Mg — Outmost core radius:1.058 A; Valence electrons: $2p^6$, $3s^2$
  - Si — Outmost core radius: 0.953 A; Valence electrons: $3s^2$ $3p^2$
  - O — Outmost core radius: 0.820 A; Valence electrons: $3s^2$ $3p^4$
- k-points (Monkhorst-Pack grid) : 3x2x3
- Plane-wave cut-off: 600 eV (energy convergence to better than 0.5 meV/atom)
- Vacuum buffer: 6 A

GSF calculations - supercells

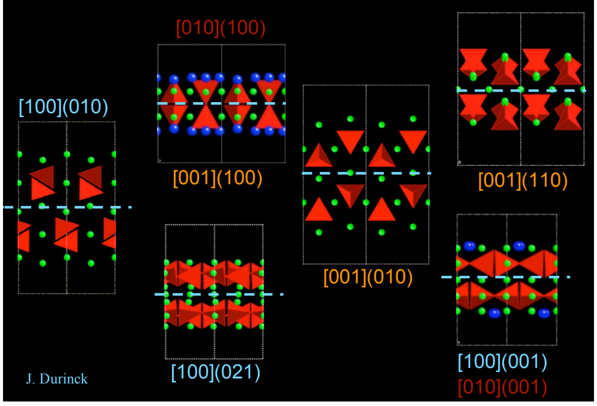

Unrelaxed GSF

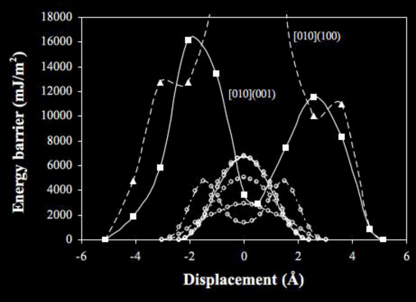

Durinck et al. (2005)

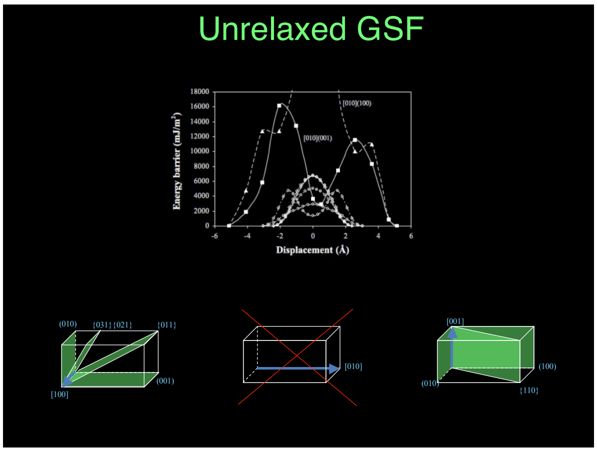
Unrelaxed GSF
Energy barrier (mJ/m²)
Displacement (Å)
[010](100)
[010](001)

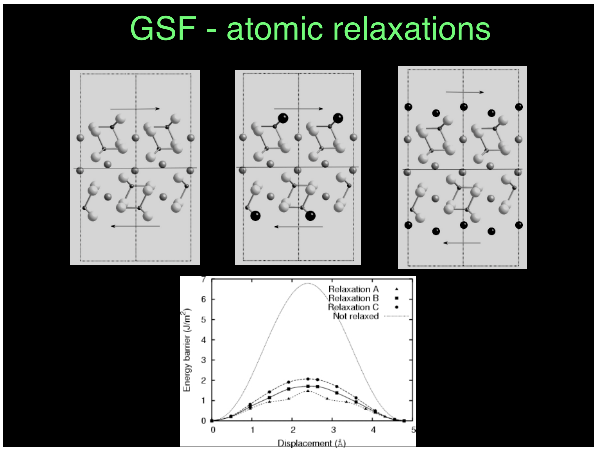
GSF - atomic relaxations
Relaxation A
Relaxation B
Relaxation C
Not relaxed
Energy barrier (J/m²)
Displacement (Å)

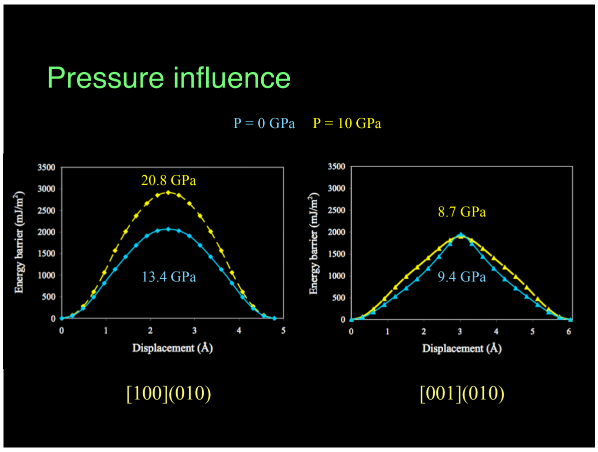
Pressure influence
P = 0 GPa
P = 10 GPa
20.8 GPa
13.4 GPa
8.7 GPa
9.4 GPa
Energy barrier (mJ/m²)
Displacement (Å)
[100](010)
[001](010)

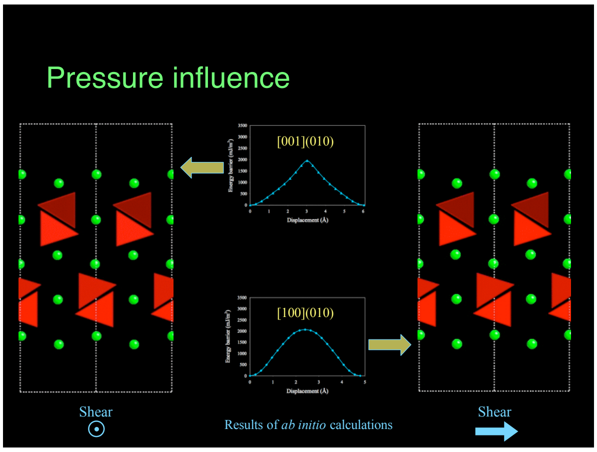
Pressure influence
[001](010)
[100](010)
Shear
Results of ab initio calculations
Shear

Pressure influence

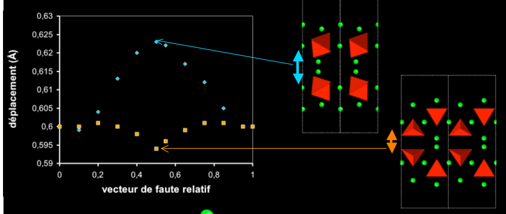

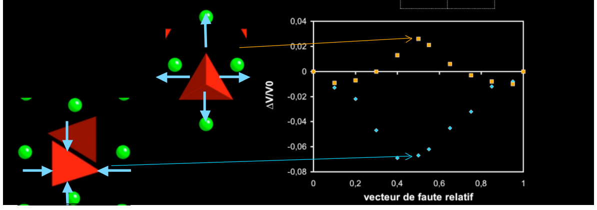

From GSF to dislocations: the Peierls model

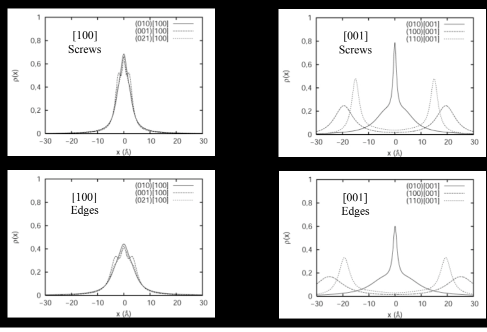

[001] screw dislocation in forsterite

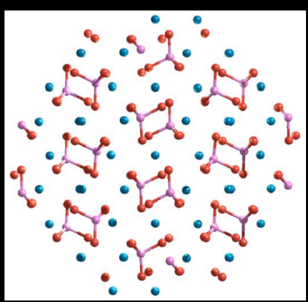

Andrew Walker

Plasticity at the mesoscopic scale

(J. Durinck - coll Devincre & Kubin, ONERA)

3D Dislocation dynamics

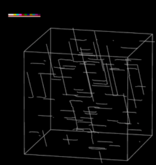

Collective behaviour

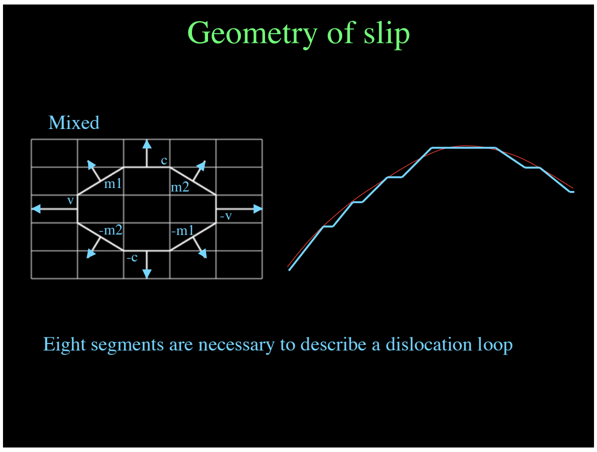
Geometry of slip
Mixed
c
m1
m2
v
-v
-m2
-m1
-c
Eight segments are necessary to describe a dislocation loop

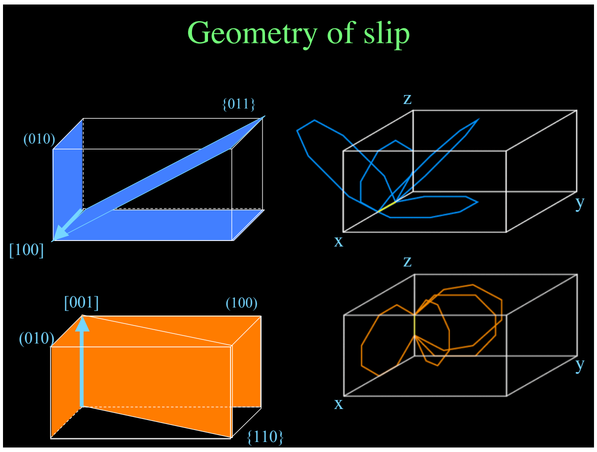
Geometry of slip
{011}
(010)
[100]
[001]
(100)
(010)
{110}
z
x
y
z
x
y

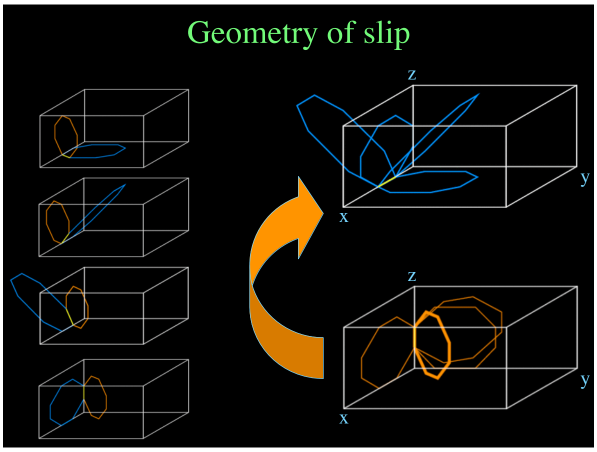
Geometry of slip
z
x
y
z
x
y

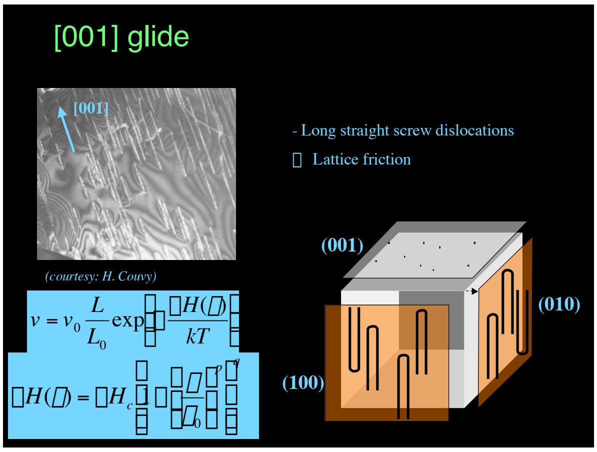
[001] glide
[001]
(courtesy: H. Couvy)
- Long straight screw dislocations
Lattice friction
$v = v_0 \frac{L}{L_0} \exp\left(-\frac{\Delta H(\tau)}{kT}\right)$
$\Delta H(\tau) = \Delta H_c \left[1 - \left(\frac{\tau}{\tau_0}\right)^p\right]^q$
(001)
(010)
(100)

Mechanical data and dislocation mobility determination: [001] dislocations

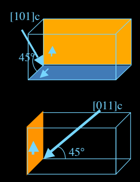

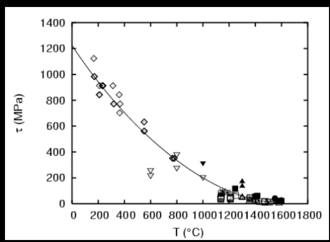

$$\Delta H(\tau) = \Delta H_c \left[1 - \left(\frac{\tau}{\tau_0}\right)^p\right]^q \xrightarrow[\Delta H_c = CkT_a]{\Delta H = CkT} \frac{T}{T_a} = \left[1 - \left(\frac{\tau}{\tau_0}\right)^p\right]^q$$

Mechanical data and dislocation mobility determination: [100] dislocations

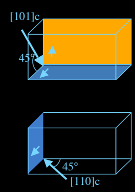

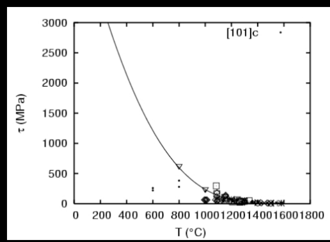

$$\Delta H(\tau) = \Delta H_c \left[1 - \left(\frac{\tau}{\tau_0}\right)^p\right]^q \xrightarrow[\Delta H_c = CkT_a]{\Delta H = CkT} \frac{T}{T_a} = \left[1 - \left(\frac{\tau}{\tau_0}\right)^p\right]^q$$

Olivine: dislocation dynamics

Case of single slip on [001](100)

- Initial population of edge dislocations: $\rho = 10^{10}$ m^{-2}
- Uniaxial extension test at constant strain rate 10^{-5}s^{-1}
- Screw mobilities : $v = v_0 \frac{L}{L_0} \exp\left(-\frac{\Delta H(\tau)}{kT}\right)$
- Sdge mobilities : $v = K.v_{vis}$

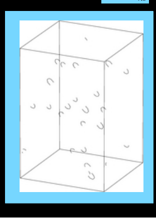

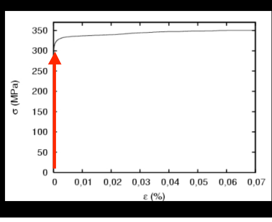

Olivine: dislocation dynamics

Case of single slip on [001](100)

- Initial population of edge dislocations: $\rho = 10^{10}$ m^{-2}
- Uniaxial extension test at constant strain rate 10^{-5}s^{-1}
- Screw mobilities : $v = v_0 \frac{L}{L_0} \exp\left(-\frac{\Delta H(\tau)}{kT}\right)$
- Sdge mobilities : $v = K.v_{vis}$

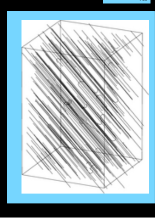

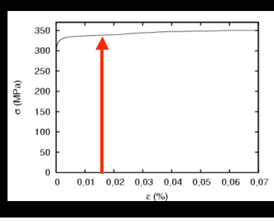

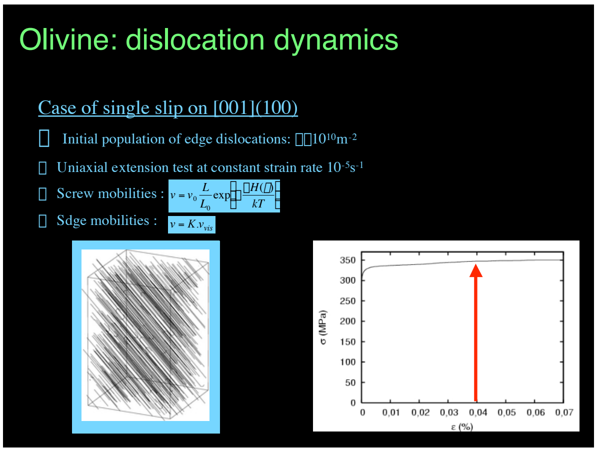
Olivine: dislocation dynamics
Case of single slip on [001](100)
Initial population of edge dislocations: $10^{10} m^{-2}$
Uniaxial extension test at constant strain rate $10^{-5} s^{-1}$
Screw mobilities :
Sdge mobilities :
$v = K.v_{vis}$
σ (MPa)
ε (%)

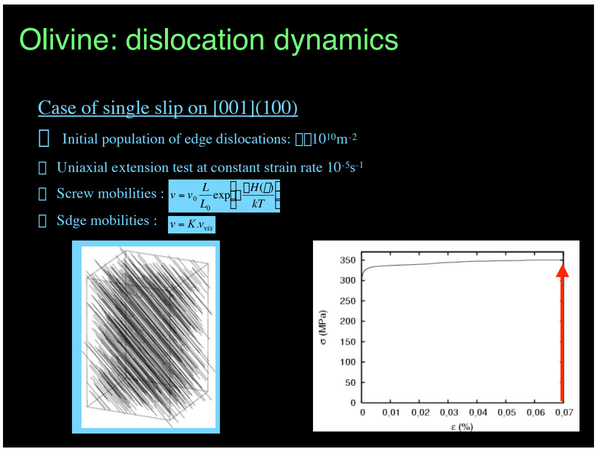
Olivine: dislocation dynamics
Case of single slip on [001](100)
Initial population of edge dislocations: $10^{10} m^{-2}$
Uniaxial extension test at constant strain rate $10^{-5} s^{-1}$
Screw mobilities :
Sdge mobilities :
$v = K.v_{vis}$
σ (MPa)
ε (%)

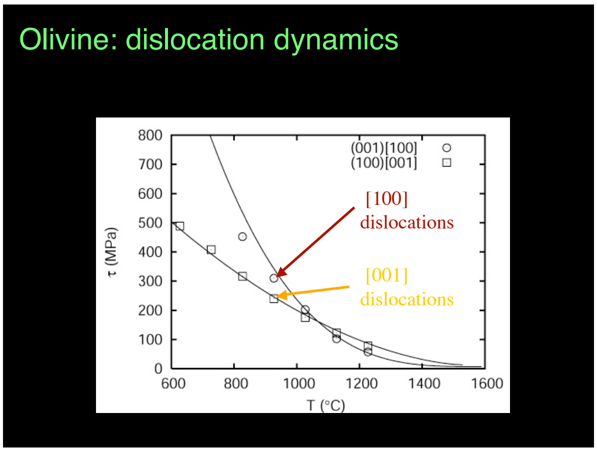
Olivine: dislocation dynamics
(001)[100]
(100)[001]
[100]
dislocations
[001]
dislocations
τ (MPa)
T (°C)

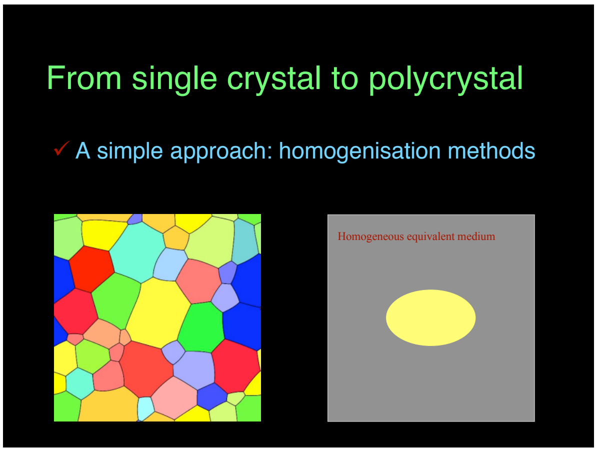
From single crystal to polycrystal
✓ A simple approach: homogenisation methods
Homogeneous equivalent medium

Visco Plastic Self-Consistent Models (VPSC)

- ✓ Very robust for CPO calculations

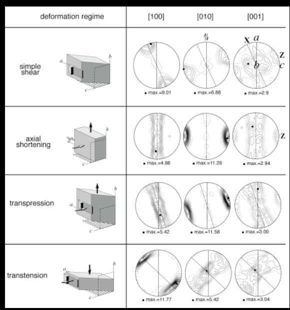

A. Tommasi

Visco Plastic Self-Consistent Models (VPSC)

- ✓ CPO in olivine

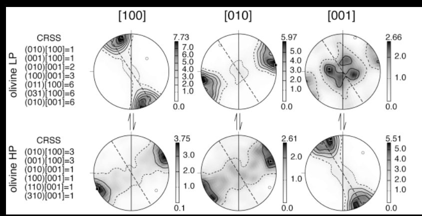

A. Tommasi

Going to mantle scale ?

(coll Mainprice & Tommasi, Montpellier)

Linking textures…

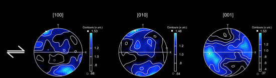

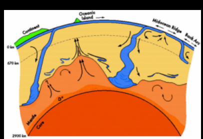

… to seismic anisotropy

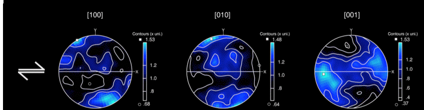

Crystal preferred orientations

Seismic properties

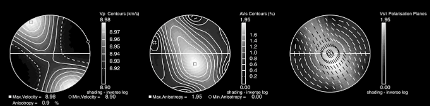

Weak anisotropy of V_P (0.9%) and V_S (1.9%)

Mainprice, Tommasi, Couvy, Cordier & Frost (2005) Nature 433, 731-733

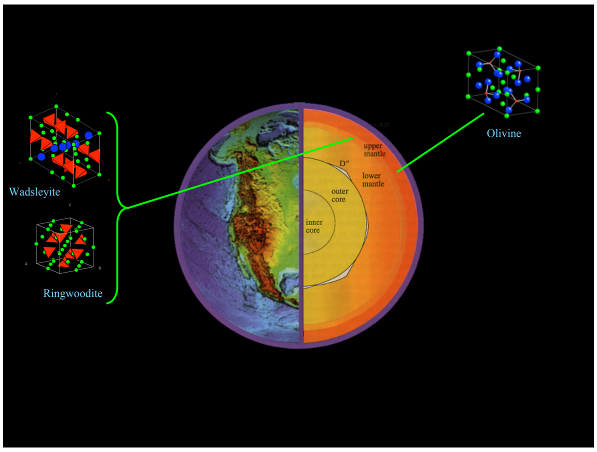
Wadsleyite
Ringwoodite
Olivine
upper mantle
D''
lower mantle
outer core
inner core

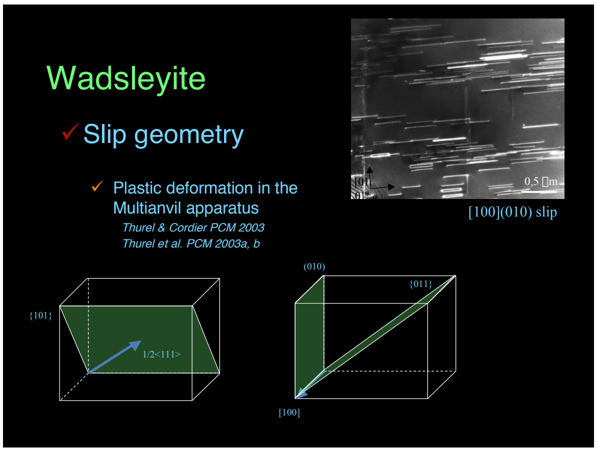
Wadsleyite
Slip geometry
Plastic deformation in the Multianvil apparatus
Thurel & Cordier PCM 2003
Thurel et al. PCM 2003a, b
[100](010) slip
{101}
1/2<111>
(010)
{011}
[100]

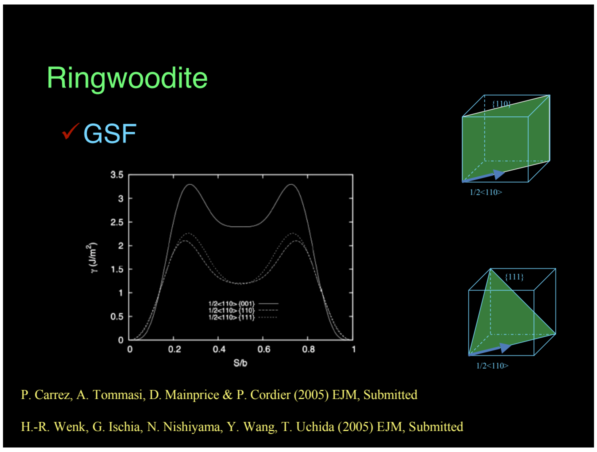
Ringwoodite
GSF
γ (J/m²)
S/b
1/2<110> (001)
1/2<110> {110}
1/2<110> {111}
{110}
1/2<110>
{111}
1/2<110>
P. Carrez, A. Tommasi, D. Mainprice & P. Cordier (2005) EJM, Submitted
H.-R. Wenk, G. Ischia, N. Nishiyama, Y. Wang, T. Uchida (2005) EJM, Submitted

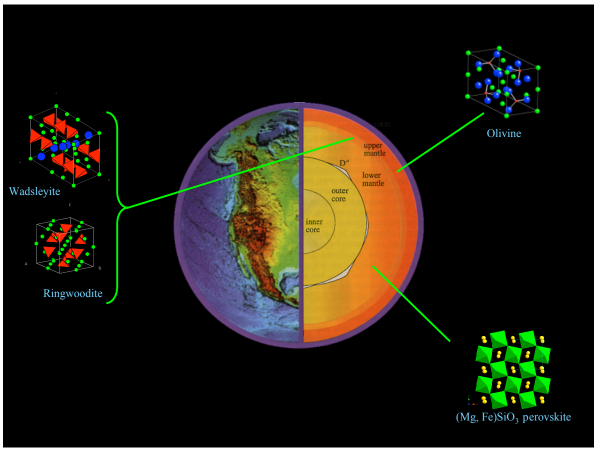
Wadsleyite
Ringwoodite
Olivine
upper mantle
D''
lower mantle
outer core
inner core
(Mg, Fe)SiO3 perovskite

$MgSiO_3$ perovskite

Deformation experiment performed at: 25 GPa - 1400°C

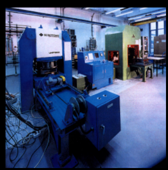

Bayerisches Geoinstitut

$MgSiO_3$ perovskite

Deformation experiment performed at: 25 GPa - 1400°C

Shear bands

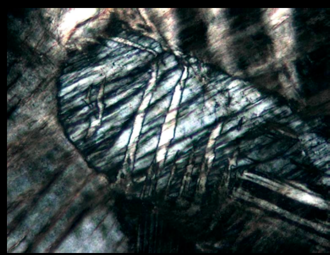

$MgSiO_3$ perovskite

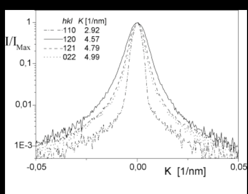

x-ray peak broadening

Slip systems:

- ✓[010](001)
- ✓[100](001)

Cordier, Ungár, Zsoldos & Tichy (2004) Nature 428, 837-840

$MgSiO_3$ perovskite: plastic shear anisotropy

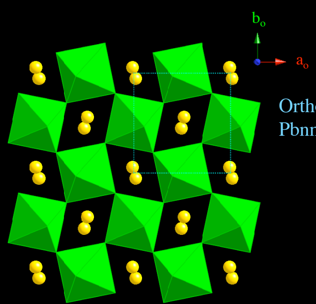

Orthorhombic
Pbnm

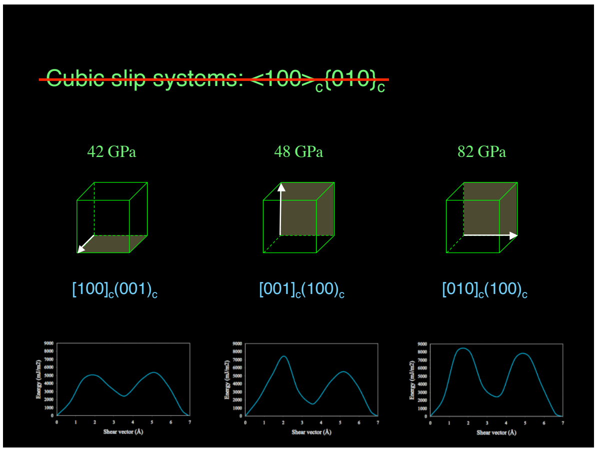
~~Cubic slip systems: <100>c{010}c~~
42 GPa
48 GPa
82 GPa
[100]c(001)c
[001]c(100)c
[010]c(100)c
Shear vector (Å)

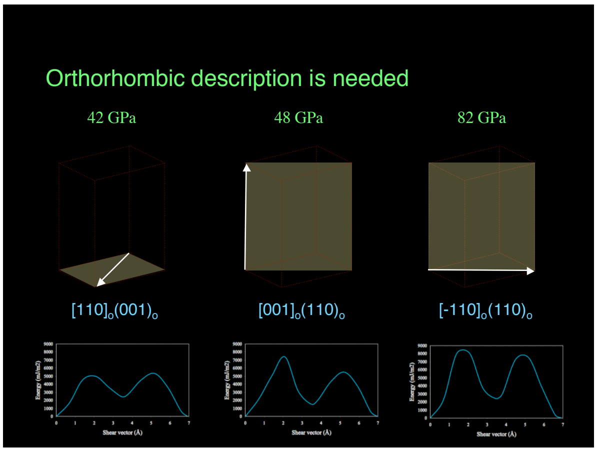
Orthorhombic description is needed
42 GPa
48 GPa
82 GPa
[110]o(001)o
[001]o(110)o
[-110]o(110)o
Shear vector (Å)

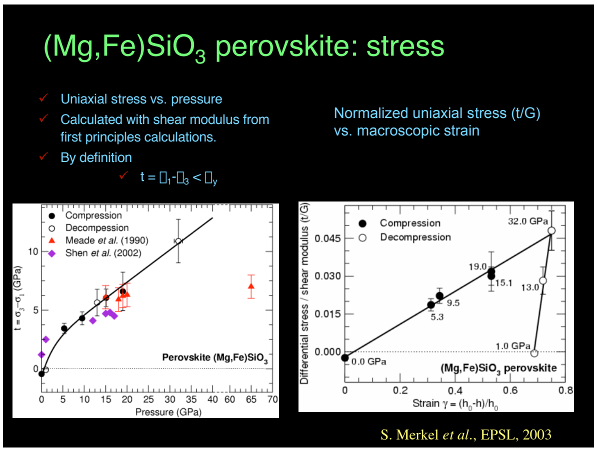
(Mg,Fe)SiO3 perovskite: stress
Uniaxial stress vs. pressure
Calculated with shear modulus from first principles calculations.
By definition
t = □1-□3 < □y
Normalized uniaxial stress (t/G) vs. macroscopic strain
Compression
Decompression
Meade et al. (1990)
Shen et al. (2002)
Perovskite (Mg,Fe)SiO3
Pressure (GPa)
32.0 GPa
19.0
15.1
13.0
9.5
5.3
1.0 GPa
0.0 GPa
(Mg,Fe)SiO3 perovskite
Differential stress / shear modulus (t/G)
Strain γ = (h0-h)/h0
S. Merkel et al., EPSL, 2003

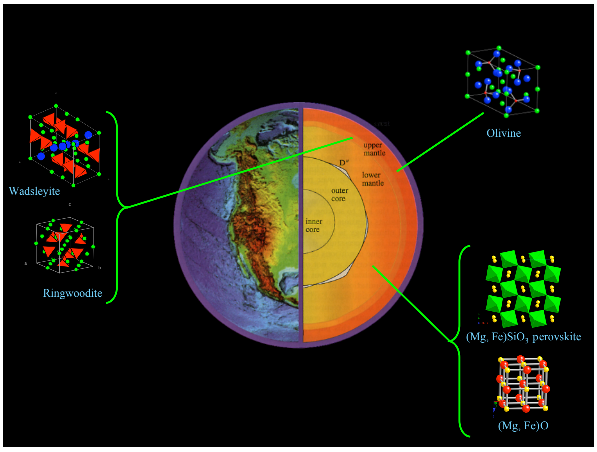
Wadsleyite
Ringwoodite
Olivine
upper mantle
lower mantle
D"
outer core
inner core
(Mg, Fe)SiO3 perovskite
(Mg, Fe)O

From single crystal to polycrystal

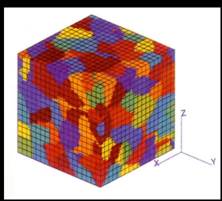

Finite elements methods

From single crystal to polycrystal

- ✓ Taking grains interactions into account

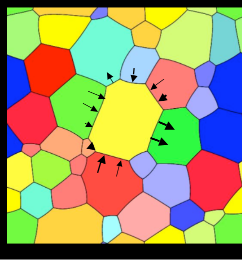

Polycrystal generation

- ✓ Voronoï polyhedra model
- ✓ Random microstructure

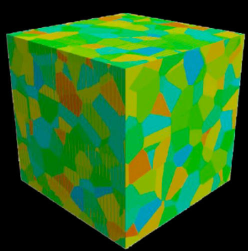

Two-phase aggregate: Pv-Mw

- ✓ 30 % Mw
- ✓ 70 % Pv

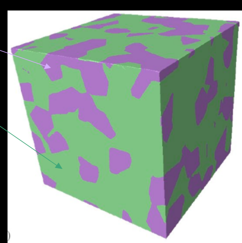

- ✓ Strong rheology contrast

Coll: K. Madi, S. Forest - Mines Paris

Two-phase aggregate: Pv-Mw

✓ 70 % Pv

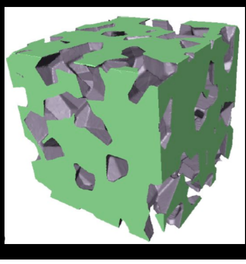

Coll: K. Madi, S. Forest - Mines Paris

Two-phase aggregate: Pv-Mw

✓ 30 % Mw

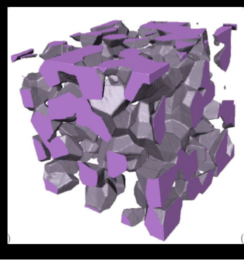

Coll: K. Madi, S. Forest - Mines Paris

Two-phase aggregate: Pv-Mw

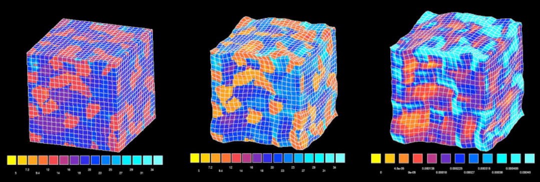

Von Mises equivalent stress

Equivalent strain

Coll: K. Madi, S. Forest - Mines Paris

Two-phase aggregate: Pv-Mw

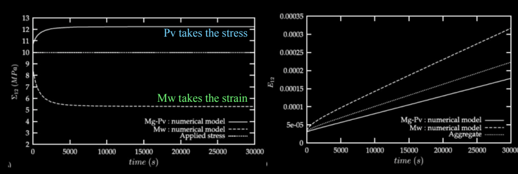

Stress

Strain

Coll: K. Madi, S. Forest - Mines Paris

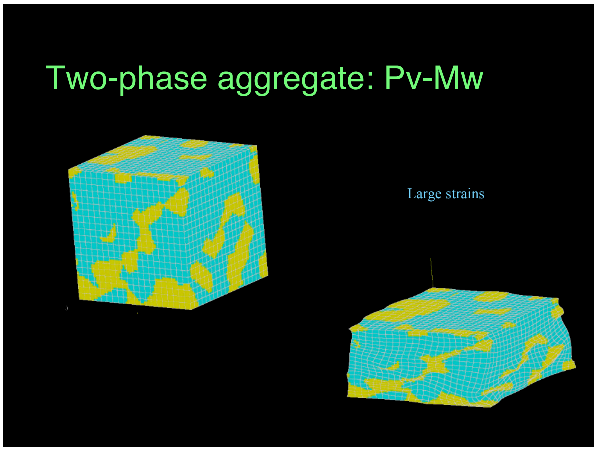
Two-phase aggregate: Pv-Mw
Large strains

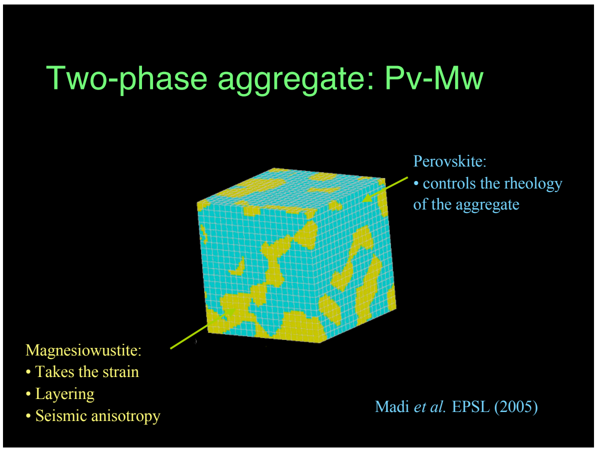
Two-phase aggregate: Pv-Mw
Perovskite:
• controls the rheology of the aggregate
Magnesiowustite:
• Takes the strain
• Layering
• Seismic anisotropy
Madi et al. EPSL (2005)

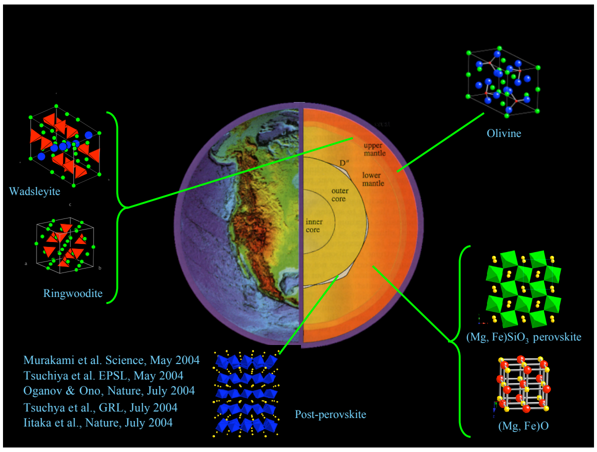
Olivine
Wadsleyite
Ringwoodite
upper mantle
lower mantle
D''
outer core
inner core
(Mg, Fe)SiO$_3$ perovskite
(Mg, Fe)O
Post-perovskite
Murakami et al. Science, May 2004
Tsuchiya et al. EPSL, May 2004
Oganov & Ono, Nature, July 2004
Tsuchya et al., GRL, July 2004
Iitaka et al., Nature, July 2004

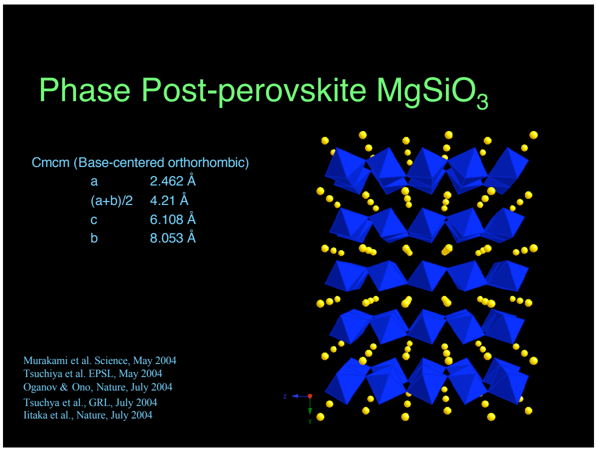
Phase Post-perovskite MgSiO$_3$
Cmcm (Base-centered orthorhombic)
a 2.462 Å
(a+b)/2 4.21 Å
c 6.108 Å
b 8.053 Å
Murakami et al. Science, May 2004
Tsuchiya et al. EPSL, May 2004
Oganov & Ono, Nature, July 2004
Tsuchya et al., GRL, July 2004
Iitaka et al., Nature, July 2004

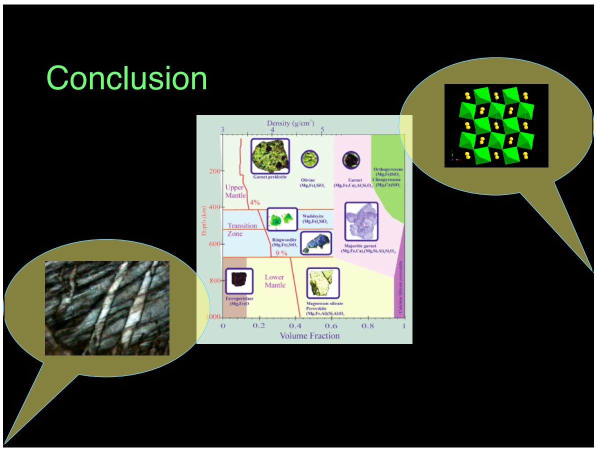
Conclusion
Upper Mantle
Transition Zone
Lower Mantle
Volume Fraction

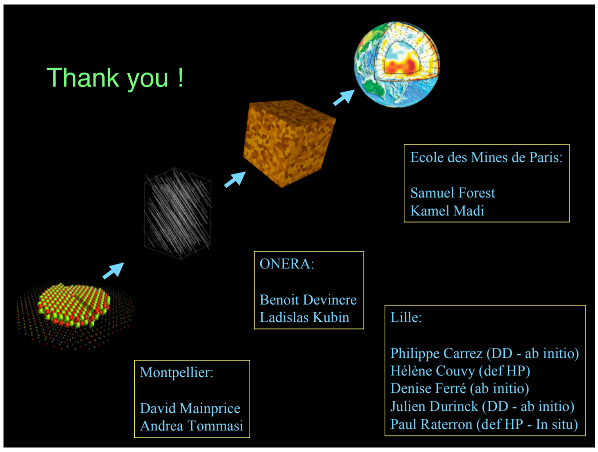
Thank you !
Ecole des Mines de Paris:
Samuel Forest
Kamel Madi
ONERA:
Benoit Devincre
Ladislas Kubin
Lille:
Philippe Carrez (DD - ab initio)
Hélène Couvy (def HP)
Denise Ferré (ab initio)
Julien Durinck (DD - ab initio)
Paul Raterron (def HP - In situ)
Montpellier:
David Mainprice
Andrea Tommasi